C^{q+} and O^{q+} vs E/A has been made and will be reported elsewhere.

The present data thus reveal striking disagreement with corresponding Z and v_i dependence features of electron continuum capture theories, and additionally provide charge-state-variation comparisons of total electron-loss cross sections with those for loss processes that populate the ~zero-degree cusp.

We gratefully acknowledge many useful conversations with C. Bottcher, J. Briggs, and S. Datz concerning related theory and experiment. This work was supported in part by the U. S. Office of Naval Research, by the National Science Foundation, and by the U. S. Department of Energy under contract with Union Carbide Corporation.

[1]G. B. Crooks and M. E. Rudd, Phys. Rev. Lett. 25, 1599 (1970); J. Macek, Phys. Rev. A 1, 235 (1970). Other theoretical work on similar subjects should be noted: W. J. B. Oldham, Jr., Phys. Rev. A 140, 1477 (1965), and 161, 1 (1967); A. Salin, J. Phys. B 2, 631, 1255 (1969), and 5, 979 (1972); K. Dettmann, K. G. Harrison, and M. W. Lucas, J. Phys. B 7, 269 (1974); Y. B. Band, J. Phys. B 7, 2557 (1974); F. Drepper and J. S. Briggs, J. Phys. B 9, 2063 (1976); J. S. Briggs, private communication, and to be published.

[2]K. G. Harrison and M. W. Lucas, Phys. Lett. 33A, 142 (1970), and 35A, 402 (1971); K. Dettmann, K. G. Harrison, and M. W. Lucas, J. Phys. B 7, 269 (1974); R. W. Cranage and M. W. Lucas, J. Phys. B 9, 445 (1976).

[3]M. G. Menendez and M. M. Duncan, in *Beam-Foil Spectroscopy*, edited by I. A. Sellin and D. J. Pegg (Plenum, New York, 1976), Vol. 2, p. 623; M. G. Menendez and M. M. Duncan, Phys. Lett. 54A, 409 (1975), and Phys. Rev. A 13, 566 (1976), and Phys. Lett. 56A, 177 (1976); M. G. Menendez, M. M. Duncan, F. L. Eisele, and B. R. Junker, Phys. Rev. A 15, 80 (1977); M. M. Duncan, M. G. Menendez, F. L. Eisele, and J. Macek, Phys. Rev. A 15, 1785 (1977); M. M. Duncan and M. G. Menendez, Phys. Rev. A 16, 1799 (1977).

[4]W. Meckbach, K. C. R. Chiu, H. H. Brongersma, and J. Wm. McGowan, J. Phys. B 10, 3255 (1977), and references therein.

[5]J. R. Macdonald and F. W. Martin, Phys. Rev. A 4, 1965 (1971).

Photon Statistics and Spectrum of Transmitted Light in Optical Bistability

R. Bonifacio[(a)] and L. A. Lugiato
Istituto di Fisica dell'Università–Milano, Milano, Italy
(Received 23 December 1977)

A quantum description of the transmitted field is given. In the bistable situation, the stationary Glauber quasi probability distribution has two peaks thereby producing a first-order phase transition. For small incident field the linewidth of the transmitted light is proportional to the atomic density and becomes very narrow as the field approaches some critical value from below. Crossing this value the spectrum splits discontinuously into a triplet (dynamical Stark shift) where the central peak is as high as twice the sidebands.

We have recently studied[1] a mean-field model, which gives the first analytical description of optical bistability[2] (OB) in the purely absorptive case for a homogeneously broadened atomic system. Although this model is quantum mechanical, in Ref. 1 it has been treated only within the semiclassical approximation. The stationary bistable behavior of the transmitted light amplitude E_T obtained by varying the incident light E_I is described by the "state equation"

$$Y = X + 2C_X/(1+X^2), \tag{1}$$

where

$$Y = \mu E_I/(\hbar^2\gamma_\perp\gamma_\parallel T)^{1/2},$$

$$X = \mu E_T/(\hbar^2\gamma_\perp\gamma_\parallel T)^{1/2},$$

$$C = \gamma_0\rho L\lambda^2/16\pi\gamma_\perp T .$$

μ is the modulus of the dipole moment of the two-level atoms, $\gamma_\parallel = T_1^{-1}$ and $\gamma_\perp = T_2^{-1}$ are the homogeneous atomic relaxation rates, γ_0 is the natural linewidth of the atoms, ρ is the atomic density, λ is the wavelength of the incident field, L is the length of the cavity, and T is the transmittivity coefficient of the mirrors. The incident field is assumed coherent, monochromatic, and perfectly tuned to the atomic transition frequency ω_0 and to the cavity. The system is bistable for $C > 4$. The discontinuity points of the hysteresis cycle of X versus Y correspond to the extrema Y_M and Y_m of the function $Y(X)$ defined by Eq. (1). For $C \gg 1$ one has $Y_M \simeq C$, $X_M \simeq 1$, $Y_m \simeq (8C)^{1/2}$, $X_m \simeq (2C)^{1/2}$ (see Fig. 1). On the basis of our model we have given also several new predictions. In particular, the spectrum of the fluorescent light is shown to exhibit a spectacular hysteresis cycle, with a sudden transition from a single narrow line to a triplet (discontinuous dynamical Stark shift).

In this Letter we report on the results of the *fully quantum mechanical* analysis of our model. These results concern the photon statistics and the spectrum of the transmitted light. We systematically distinguish between the case of a good-quality cavity ($K \ll \gamma_\perp, \gamma_\parallel$, where $K = cT/2L$ is the cavity damping constant) and the case of a bad-quality cavity ($K \gg \gamma_\perp, \gamma_\parallel$). We finally discuss the spectrum of the fluorescent light.

(1) *Photon statistics of the transmitted light.* —Case (a) $K \ll \gamma_\perp, \gamma_\parallel$: We adiabatically eliminate the atomic variables by following the general method devised by Lugiato.[3] We obtain a closed time-evolution equation for the Glauber quasi probability distribution of the field $P(X, X^*, t)$ which contains derivatives of all orders in X, X^*. The drift term of this equation is intimately connected with Eq. (1). We have calculated exactly the stationary distribution $P_{st}(|X|)$, which vanishes for $|X| \geq Y$ because the transmitted field cannot exceed the incident field. For $|X| \leq Y$ one finds

$$P_{st}(|X|) = \mathfrak{N} \exp\{-4N_s[\tfrac{1}{2}|X|^2 + \ln|X| + 2C\ln(Y - |X|)]\}, \tag{2}$$

where $\mathfrak{N}$ is a suitable normalization constant and $N_s^{-1} = 8\pi\omega_0\hbar\mu^2/(\gamma_\perp\gamma_\parallel V)$ is the saturation photon number, with V the volume of the cavity. The maxima of distribution (2) coincide with the solutions of Eq. (1) which are stable according to the linear stability analysis. Hence for $C > 4$ and $Y_m < Y < Y_M$ distribution (2) has two peaks of different widths and heights. One obtains a picture which resembles first-order phase transitions in equilibrium systems. In fact, as shown by Fig. 1, $\langle|X|\rangle_s$ coincides with one of the two semiclassical solutions everywhere except in a narrow transition region. The center of this region is that value of Y in correspondence of which the two peaks of distribution (2) have equal areas. The larger is the quantity N_s/C, the narrower is the transition region. In the limit $N_s/C \to \infty$ one obtains an infinitely sharp transition, i.e., a Maxwell rule. However, it does not coincide with the Maxwell rule of equilibrium thermodynamics. In fact, in the analogy between our system and a liquid-vapor system, Y corresponds to the pressure while X corresponds to the volume.[4] Now the Maxwell rule that we obtain does not coincide with the prescription $\oint_\Gamma Y dX = 0$, where the path Γ is indicated by the arrows in Fig. 1. By means of Fig. 1 we can decide which of the two semiclassical solutions is absolutely stable and which is metastable. In fact, for each value of Y satisfying $Y_m < Y < Y_M$ the stable solution practically coincides with $\langle|X|\rangle_s$. By suitably generalizing the method of Kramers,[5] we have calculated the transition rates from one semiclassical solution to the other. It turns out that if N_s/C is large, the lifetime of the metastable states is extremely long. Note in Fig. 2 the remarkable peak of fluctuations in the transition region. This behavior arises from the strong competition between two peaks of comparable areas.

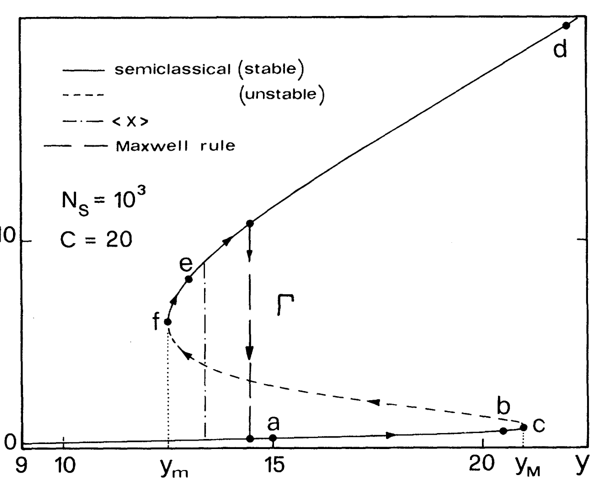

FIG. 1. The mean value of the transmitted field $\langle X\rangle$ is compared with the semiclassical hysteresis cycle and with the Maxwell construction Γ. The spectrum of the transmitted light in correspondence to points a–f is plotted in Fig. 3.

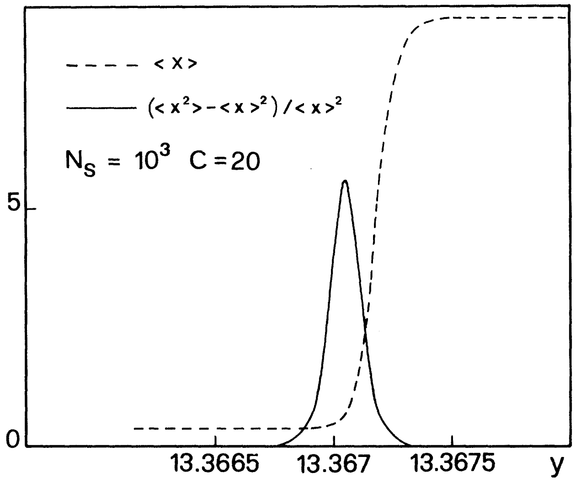

FIG. 2. Mean value and relative fluctuation of the transmitted field.

Case (b) $K \gg \gamma_\perp, \gamma_\parallel$: We adiabatically eliminate the field variables thereby obtaining a Fokker-Planck equation for a suitable quasi probability distribution of the atomic variables.[6] The stationary solution of this equation can be calculated only approximately. One obtains results for the photon statistics which are qualitatively similar to those described in the case $K \ll \gamma_\perp, \gamma_\parallel$.

(2) *Spectrum of the transmitted light* $S(\omega)$.—It is proportional to the Fourier transform of the time correlation function in steady state, $\langle A^\dagger(t) \times A\rangle_s$, where $A^\dagger$ is the creation operator of photons of the transmitted field. Subdividing $A(t)$ into the stationary mean value $\langle A\rangle$ and the fluctuation $\delta A(t) = A(t) - \langle A\rangle$, we have that $S(\omega)$ is composed of a coherent and an incoherent part $S(\omega) = S_{\text{coh}}(\omega) + S_{\text{inc}}(\omega)$, with $S_{\text{coh}}(\omega) = |\langle A\rangle|^2 \delta(\omega - \omega_0)$. To evaluate $S(\omega)$ we neglect the transitions from one semiclassical solution to the other, thereby treating stable and metastable states on the same footing. Hence we can replace $|\langle A\rangle|^2$ in $S_{\text{coh}}(\omega)$ by $N_s X^2$, where X is the solution of Eq. (1) which we are considering.

Case (a) $K \ll \gamma_\perp, \gamma_\parallel$: The linewidth is scaled by the empty-cavity half-width K. We linearize the time-evolution equation for $P(X, X^*, t)$ around the steady state. Setting $\nu = \omega - \omega_0$, we obtain

$$S_{\text{inc}}(\omega) = \{CKX^2/[2\pi(1+X^2)]\}[(1+X^2)^{-1}(\nu^2 + K^2\bar{\lambda}^2)^{-1} + (\nu^2 + K^1\lambda_\varphi^2)^{-1}], \tag{3}$$

where $\bar{\lambda} = dY/dX$ and $\lambda_\varphi = Y/X$. Hence $S_{\text{inc}}(\omega)$ is always a single line and changes discontinuously at $Y = Y_M, Y_m$. For $C \gg 1$, $\bar{\lambda}$ and λ_φ are roughly equal except in the neighborhood of $Y = Y_M, Y_m$ where $\bar{\lambda}$ tends to zero. Hence approaching these points one finds a line narrowing. Note that for $Y \geqslant Y_M \gg 1$ one has $X \simeq Y$ so that $\bar{\lambda} \simeq \lambda_\varphi \simeq 1$ and the linewidth coincides with the empty-cavity width. On the other hand, for $Y \ll Y_M$, $C \gg 1$, one has $X \ll 1$ so that $\bar{\lambda} \simeq \lambda_\varphi \simeq 2C$. Hence the linewidth is much larger than the empty-cavity width and is proportional to the atomic density (cooperative broadening effect).

Case (b) $K \gg \gamma_\perp, \gamma_\parallel$[7]: The linewidth is scaled by the atomic rates $\gamma_\perp, \gamma_\parallel$. By linearizing the Fokker-Planck equation we have that $S_{\text{inc}}(\omega)$ depends on the three damping constants λ_φ and

$$\lambda_\pm = \tfrac{1}{2}\{\gamma_\parallel/\gamma_\perp + Y/X \pm [(\gamma_\parallel/\gamma_\perp - Y/X)^2 - 4X(\gamma_\parallel/\gamma_\perp)(2X - Y)]^{1/2}\}. \tag{4}$$

One finds

$$S_{\text{inc}}(\omega) = \{C\gamma_\perp^2 X^2/[2\pi K(1+X^2)]\}[(\nu^2 + \gamma_\perp^2\lambda_\varphi^2)^{-1} + F(\nu)]. \tag{5}$$

More specifically, when $\lambda_\pm$ are real, one gets $F(\nu) = f_-(\nu) - f_+(\nu)$, where

$$f_\pm(\nu) = [(\lambda_+^2 - \lambda_-^2)(\nu^2 + \gamma_\perp^2\lambda_\pm)]^{-1}[(\gamma_\parallel/\gamma_\perp)^2(1+X^2) - \lambda_\pm^2]. \tag{6}$$

For $Y \ll Y_M$, $C \gg 1$, one has that $\lambda_\varphi \simeq \lambda_+ \simeq 2C$, $\lambda_- \simeq \gamma_\parallel/\gamma_\perp$. The contribution from $f_-(\nu)$ is negligible, so that the half-width of the spectrum is the cooperative linewidth $\gamma_R = 2\gamma_\perp C$ which is proportional to the atomic density. On the contrary, approaching the discontinuity points $Y = Y_M, Y_m$, the contribution $f_-(\nu)$ dominates because $\lambda_- \to 0$, so that one has a line narrowing. When $\lambda_\pm$ are complex, by putting $\lambda_\pm = \lambda_1 \pm i\lambda_2$ one has $F(\nu) = g(\nu) + g(-\nu)$, where

$$g(\nu) = \{2(\lambda_1^2 + \lambda_2^2)[(\nu - \gamma_\perp\lambda_2)^2 + \gamma_\perp^2\lambda_1^2]\}^{-1}$$
$$\times \{\lambda_1^2 + \lambda_2(\nu/\gamma_1 - \lambda_2) + (1 - \nu/2\lambda_2\gamma_\perp)[(\gamma_\parallel/\gamma_\perp)^2(1+X^2) + \lambda_2^2 - \lambda_1^2]\}. \tag{7}$$

When $Y \geqslant Y_M \gg 1$ one has $X \simeq Y$, $\lambda_1 \simeq \tfrac{1}{2}(1 + \gamma_\parallel/\gamma_\perp)$, $\lambda_2 \simeq Y(\gamma_\parallel/\gamma_\perp)$.$^{1/2}$ Hence $S_{\text{inc}}(\omega)$ reduces to the superposition of three Lorentzians: The central peak at $\omega = \omega_0$ has width $2\gamma_\perp$ and the symmetrical sidebands at $\omega = \omega_0 \pm \mu E_I/\hbar$ have width $\gamma_\perp + \gamma_\parallel$. The ratio of the height of central peak to the height of sidebands

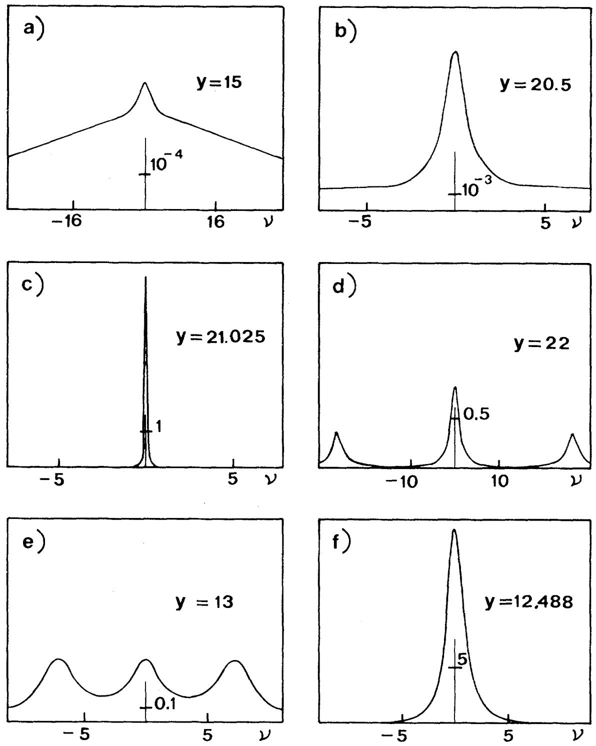

FIG. 3. Hysteresis cycle of the incoherent part of the spectrum $S_{\rm inc}$ of the transmitted light for $\gamma_\parallel = 2\gamma_\perp \ll K$ and $C = 20$. The frequency ν is expressed in units $\gamma_\perp$ and $S_{\rm inc}$ in units $C/2\pi K$. The scale varies from diagram to diagram as indicated. The points of the X-Y plane corresponding to (a)–(f) are indicated in Fig. 1.

is 2 instead of 3 as in resonance fluorescence.[8] Therefore crossing the discontinuity point $Y = Y_M$ one has a discontinuous dynamical Stark shift. The hysteresis cycle of $S_{\rm inc}(\omega)$ for $K \gg \gamma_\perp, \gamma_\parallel$ is shown in Fig. 3.

(3) *Spectrum of the fluorescent light* $I(\omega)$.—It is proportional to the Fourier transform of

$$\sum_{i=1}^{N} \langle r_i^{\,+}(t) r_i^{\,-}\rangle_s ,$$

where N is the number of atoms and $r_i^{\,+}$ is the raising operator of the ith two-level atom. Subdividing $r_i^{\,+}(t)$ into the stationary mean value $\langle r_i^{\,+}\rangle$ and the fluctuation $\delta r_i^{\,+}(t) = r_i^{\,+}(t) - \langle r_i^{\,+}\rangle$, we have that $I(\omega) = I_{\rm coh}(\omega) + I_{\rm inc}(\omega)$, where

$$I_{\rm coh}(\omega) = (N\gamma_\parallel X^2/4\gamma_\perp)(1+X^2)^{-2}\delta(\omega-\omega_0). \qquad (8)$$

The integrated fluorescence spectrum $J = \int d\omega\, I(\omega)$ is by definition equal to the population of the upper level. Using Eq. (8) one finds that $J_{\rm coh}/J_{\rm inc} = (2\gamma_\perp/\gamma_\parallel)(1 + X^2 - \gamma_\parallel/2\gamma_\perp)$. Hence for $\gamma_\parallel \simeq \gamma_\perp$, $C \gg 1$, the incoherent part is negligible in the low-transmission branch, whereas it is dominant in the high-transmission branch. Making a proper regression *Ansatz*, $I_{\rm inc}(\omega)$ turns out to be the same as calculated in Ref. 4, provided that $K \gg \gamma_\perp, \gamma_\parallel$, $\gamma_\parallel = 2\gamma_\perp$. These results agree with the predictions of Ref. 1. $I_{\rm inc}(\omega)$ behaves roughly as $S_{\rm inc}(\omega)$ but with a ratio 3:1 between the height of the central peak and that of the sidebands in the case of Fig. 3(d). The total incoherent part of the transmitted light has the same order of magnitude of the fraction of fluorescent light emitted in each diffraction solid angle $\lambda^2 L/V$.

A detailed derivation of the results described in this Letter will be given elsewhere.[9] This work was partially supported by the European Research Organization under Grant No. DA-ERO-77-G-054, and by Consiglio Nazionale delle Ricerche, Italy.

Note added.—We have recently given a rigorous justification of the mean-field approximation from Maxwell-Bloch equations in the double limit $\alpha L \to 0$ and $T \to 0$ with $\alpha L/2T = C$ fixed and arbitrary. In practice the mean-field approximation is good except for high values of αL. [See R. Bonifacio and L. A. Lugiato, "Bistable Absorption in a Ring Cavity" (to be published).] Furthermore, we have demonstrated that a large part of the upper branch of the bistable region of Fig. 1 is unstable due to propagation effects, so that self-pusling can be expected. [R. Bonifacio and L. A. Lugiato, "Instabilities for a Coherently Driven Absorber in a Ring Cavity" (to be published).]

[(a)]Also at Istituto Nazionale di Ottica, Firenze, Italy.

[1]R. Bonifacio and L. A. Lugiato, Opt. Commun. 19, 172 (1976), and Phys. Rev. A (to be published).

[2]S. L. McCall, Phys. Rev. A 9, 1515 (1974), and references quoted therein; H. M. Gibbs, S. L. McCall, and T. N. C. Venkatesan, Phys. Rev. Lett. 36, 1135 (1976).

[3]L. A. Lugiato, Physica (Utrecht) 81A, 565 (1975), and 82A, 1 (1976).

[4]G. S. Agarwal, L. M. Narducci, Da Hsuan Feng, and R. Gilmore, in Proceedings of the Fourth Rochester Conference on Coherence and Quantum Optics, June, 1977 edited by L. Mandel and E. Wolf (Plenum, New York, to be published).

[5]H. A. Kramers, Physica (Utrecht) 7, 284 (1940).

[6]H. Haken, in *Handbuch der Physik*, edited by S. Flügge (Springer, Berlin, 1970), Vol. 25/2c.

[7]Similar results for the spectrum of the transmitted light in the case $K \gg \gamma_\perp$, $\gamma_\parallel = 2\gamma_\perp$ have been contempo-

rarily and independently obtained by G. S. Agarwal, L. M. Narducci, Da Hsuan Feng, and R. Gilmore via a somehow different approach.

[8]B. R. Mollow, Phys. Rev. 188, 1969 (1969).
[9]R. Bonifacio, M. Gronchi, and L. A. Lugiato, to be published.

"Sputtering" of Ice by MeV Light Ions

W. L. Brown, L. J. Lanzerotti, J. M. Poate, and W. M. Augustyniak
Bell Laboratories, Murray Hill, New Jersey 07974
(Received 11 January 1978)

We have measured the rate of erosion of thin films of water ice at low temperatures by bombardment with MeV hydrogen, helium, carbon, and oxygen ions. The effective "sputtering coefficients" are orders of magnitude higher than those anticipated from conventional sputtering theories. For example, for helium at 1.5 MeV, ~ 10 H_2O molecules are removed for each incident ion. We believe that the erosion process is closely associated with atomic ejection following ionization in the region near the surface.

Sputtering of metallic or covalent bonded solids is now a rather well understood phenomenon[1] with material being ejected from the surface as a result of the nuclear collision cascades set up in the solid. The situation is very different for ionic solids, such as alkali halides,[2,3] where the amount of sputtered material does not appear to depend on the nuclear stopping processes. There is a paucity of experimental information on the sputtering of condensed gases[4]—a subject of considerable astronomical importance. Radiation damage and channeling in ice crystals have previously been studied,[5] but without observation of the erosion phenomena reported in this paper. Erosion effects have apparently been observed in studies of the energy loss of MeV light ions through thin frozen films of Ar, N_2, and O_2,[6] but have not been quantitatively determined. In this paper we present the first measurements on the sputtering or erosion coefficients of water ice by energetic particles.

We have used Rutherford backscattering and thin-film techniques in our experiments. A vitreous carbon surface is cooled with a Cryotip[7] helium transfer tube to controlled temperatures between 15 and 110°K. Ice is grown on this surface by admitting H_2O vapor as a broad stream from a tube which the cold surface faces. The inset to Fig. 1 shows the geometry of the experiment. A typical growth rate is ~ 600 Å/min. Films have been prepared between 250 Å and 1.5 μm in thickness in this way. Under these conditions of deposition the ice film should be amorphous[8] and our visual observations are consistent with this expectation. The films are also stable. Even at 110°K the sublimation rate of ice is less than a monolayer a day. The erosion of the films has generally been carried out with the eroding beam electrostatically swept over a 4-mm-diam aperature to produce a uniform eroded region. For backscattering analysis, the beam is collimated to 1 mm diam, and can be located to ex-

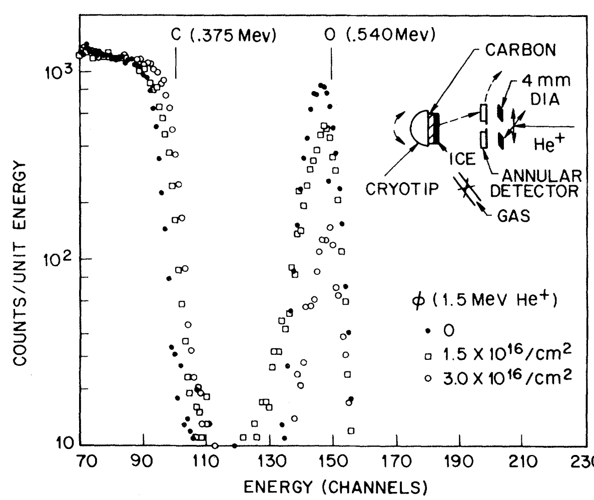

FIG. 1. Spectra of backscattered 1.5-MeV He ions from an ice film on carbon at three different stages in the erosion of the film by 1.5-MeV He ions. Erosion is carried out with a beam scanned to fill a 4-mm-diam aperture. Backscattering spectra are taken with a 1-mm detector aperture. Note that the backscatter peak from oxygen decreases with erosion and the backscattered edge for C moves to higher energy. The C and O marks indicate the energies of backscattering from C and O is they were at the surface. The energy scale is in channels of a multichannel analyzer.